Reversible resistance switching in Ge-Sb-Te thin films without amorphous-crystalline phase-change

Ramanathaswamy Pandian, Bart J. Kooi, Jasper Oosthoek, George Palasantzas, Jeff T. M. De Hosson

Department of Applied Physics, Zernike Institute for Advanced Materials, and the Materials Innovation Institute, University of Groningen, Nijenborgh 4, 9747 AG Groningen, the Netherlands.

Andrew Pauza

Plasmon Data Systems Ltd., Whiting Way, Melbourn Royston, Hertsfordshire, SG8 6EN, United Kingdom.

ABSTRACT

Apart from the resistance switching originating from the amorphous-crystalline phase-change in GeSbTe thin films, we demonstrate another switching mechanism named 'polarity-dependent resistance (PDR) switching'. The electrical resistance of the film switches between a low- and high-state when the polarity of the applied electric field is reversed. This switching is not connected to the phase-change, as it is only exhibited in crystallized parts of the film, but probably to the solid-state electrolytic behavior (i.e. high ionic conductivity) of GeSbTe under an electric field. I-V characteristics of simple capacitor-like cells of various dimensions clearly exhibited the switching behavior when sweeping the voltage between +1 V and -1 V (starting point: 0 V). The switching was demonstrated also with voltage pulses of amplitudes down to 1 V and pulse widths down to 1 microsecond for hundreds of cycles with resistance contrasts up to 150% between the resistance states. Conductive atomic force microscopy (CAFM) was used to examine PDR switching at nanoscales in tip-written crystalline marks, where the switching occurred for voltages ≤ 1.5 V with resistance contrasts > 3 orders of magnitude. The above PDR switching was observed in excess-Sb $Ge_2Sb_{2+x}Te_5$ films, but was (nearly) impossible with stoichiometric $Ge_2Sb_2Te_5$, showing the important role played by the excess Sb. Our experiments demonstrate a novel and technologically important switching mechanism, which consumes less power than the usual phase-change switching and provide the opportunity to bring together the two resistance switching types (phase-change and PDR) in a single system to extend the applicability of GeSbTe materials.

1. INTRODUCTION

For next generation nonvolatile memories, several random access memory (RAM) technologies have been proposed e.g. based on magneto-resistance (MRAM) [1], ferroelectricity (FRAM) [2], phase-change (PRAM) [3], and electrical-resistance (RRAM) [4-13]. Among them, PRAM and RRAM based on *electrical resistance switching* have been given more focus in recent years as they prove to be promising candidates for the next generation nonvolatile memories. Being the active medium of the proposed phase-change and electrical-resistance based memories, chalcogenide materials are particularly promising and versatile. PRAM is based on resistance switching caused by the transition between an amorphous and crystalline phase and is not voltage-polarity dependent. RRAM, on the other hand, is sensitive to the polarity of the applied voltage and not connected to a structural phase transformation. The resistance switching of RRAM is attributed to the electrolytic behavior and/or ionic conductivity of the material in the solid-state. Up to now, the phase-change and polarity-dependent resistance switching in chalcogenides were considered independently [14]. For example, numerous compositions derived from the GeSbTe system showed amorphous-crystalline switching and Ag- or Cu-doped chalcogenides such as AgS, CuS , AgGeSe, AgGeTe and AgInSbTe showed PDR switching [9-13]. In Ag/Cu-free chalcogenides, such as in GeSbTe system most commonly used in phase-change data storage, the PDR switching has not yet been demonstrated. AgInSbTe is the only material (comparable to GeSbTe compositions) for which the PDR switching is reported [13]. However, this system showed a high threshold voltage (>10 V), which is a significant drawback. In this paper, we demonstrate that PDR switching

could be achieved with GeSbTe, at various length scales, using low voltages (≤ 2V) incapable of inducing the amorphous-crystalline phase change in the system.

2. EXPERIMENTS

The samples analyzed consisted of 20 or 40 nm thick Sb-excess $Ge_2Sb_{2+x}Te_5$ (GST) phase-change films on 100 nm thick Mo bottom-electrodes on Si substrates. Later, and this will be explicitly mentioned below, we also analyzed stoichiometric $Ge_2Sb_2Te_5$ films. Mo and amorphous GST were deposited by DC-magnetron sputtering. The GST films were deposited on the Mo bottom electrodes without taking the samples out of the vacuum of the deposition chamber. Ag or Al was used as top-electrode contacts in capacitor-like prototype cells as shown in figure 1a. With such memory cells, the PDR switching behavior was examined via I-V measurements using a Keithley 2601 Source-Meter with a voltage sweep rate of ~0.8 V/s. When the cell is subjected to a pulse-mode operation, the DC voltage source is replaced by a pulse generator, and the switching was tested for various pulse-amplitudes and pulse widths. To investigate the switching at nanoscales, conductive atomic force microscopy (CAFM, Veeco Dimension-3100) was used. The Pt/Ir coated conductive tip of the microscope served as a top-electrode in this case. The schematic of the CAFM experimental setup is shown in figure 1b. With the setup, in addition to usual height topographs, also current-images showing the local conductivity of the sample could be obtained. Biasing the sample with smaller DC voltages (<< the threshold voltage for phase-change) and measuring the electrical current (passing along the sample thickness) with a conductive AFM-tip that is virtually grounded, gives the conductance image. A high-gain current amplifier connected electrically in series with the tip detects currents down to 5 pA. In our experimental setup, scanning the amorphous area with lower DC bias voltages (1-2 V) did not show any significant current flow above this lower limit. For the PDR switching experiments the volume of the GST film in-between the electrodes was electrically crystallized. Electrical crystallization occurs due to the Joule-heating. All the measurements were performed in air and at room temperature.

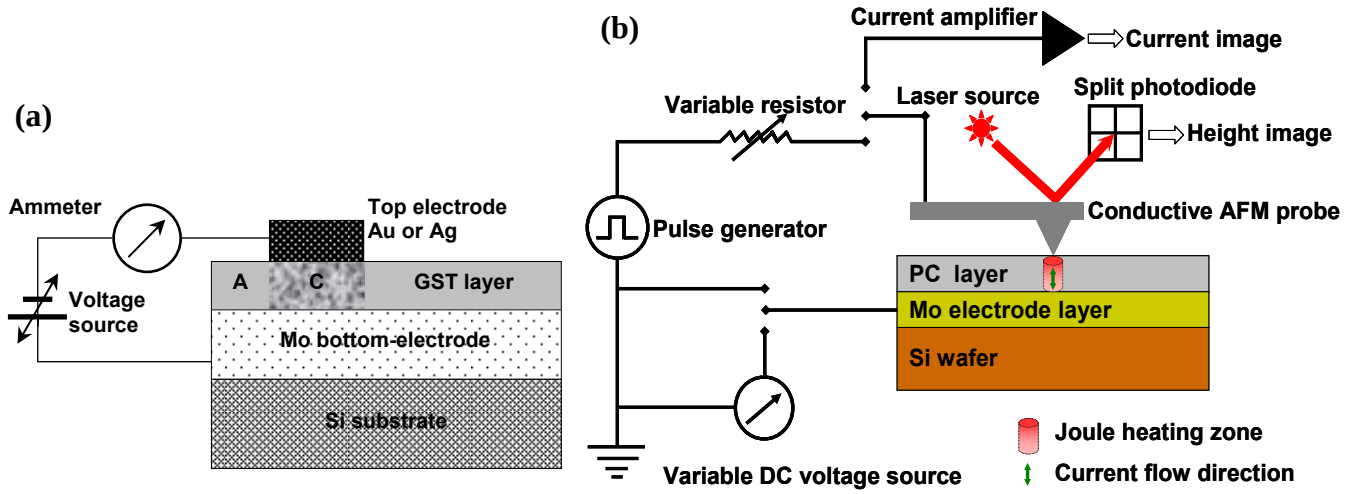

Figure 1. *(a) Schematic of capacitor-like cell structure with Ag or Al top-electrode, where A and C refers to amorphous and polycrystalline phase of the GST layer, respectively. (b) Schematic of CAFM experimental setup showing the sample structure and electronic circuit with various components.*

3. RESULTS AND DISCUSSION

PDR switching with capacitor-like cells

To investigate PDR switching at macroscopic level (millimeter scale), capacitor-like memory cells with Ag top-electrodes were prepared (size of Ag electrodes was about 1 mm and thickness was ~ 0.1 mm). Figure 2a shows a typical I-V behavior of such a prototype cell. Note that before the measurements, the amorphous GST between the electrodes was crystallized by sweeping the voltage from zero to values higher than the threshold voltage for crystallization, and PDR switching without this initial crystallization of GST turned out impossible. The sample is therefore initially in a low-resistance state (LRS). When sweeping the voltage from zero to the negative values with respect to the bottom electrode, a linear I-V behavior is observed until the voltage reaches -0.4 V. Beyond this threshold voltage ($V_{th} \approx$ -0.4 V), the sample switches to a high-resistance state (HRS), which is ~ 5 times the LRS, and remains at this state for further voltage sweep from -0.4 to -0.6, and from -0.6 to +0.4 in the other direction. Almost a linear I-V behavior is observed, at this HRS, for the voltage sweep from -0.6 to +0.4. Sweeping the voltage above +0.4 switches the sample back to its initial LRS. The cutoff for large currents above 40 mA is due to a current limit to prevent sample damage. I-V characteristic with the two different resistance states therefore clearly exhibits (see figure 2a) the PDR switching behavior of the sample. This intrinsic memory effect is reproducible for a number of cycles within ±0.4 V. The two (meta-) stable resistance states are nonvolatile for several months as tested after switching and could be read with low bias voltages ($<<V_{th}$) of either polarity.

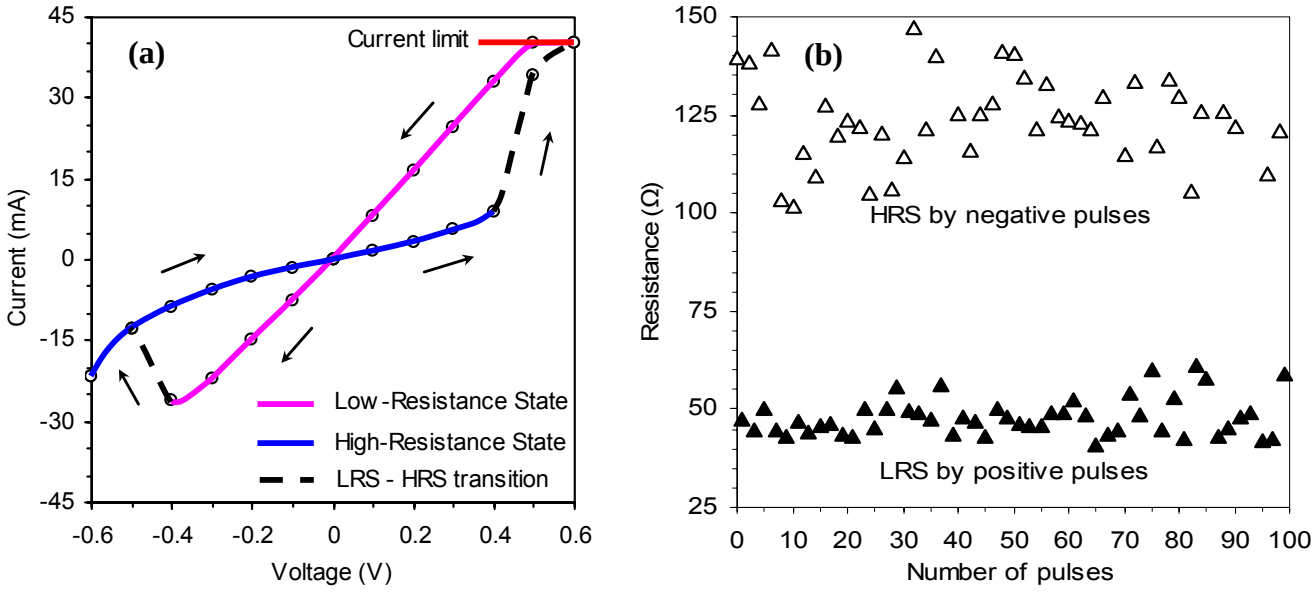

Figure 2. *(a) Memory switching I-V behavior of a cell with Ag top-electrode. (b) LRS and HRS during the pulse-mode operation with voltage pulses of ±1.25 V and 1 µs.*

Using voltage pulses for the switching includes the advantages of fast device operation and reducing thermal effects or damage. An example for the pulse-mode operation of a cell, for a number of cycles, exhibiting the two resistance states is depicted in figure 2b. Voltage pulses of ±1.25 V and 1 µs were used to perform the switching. Negative pulses yielded LRS to HRS switching, which is equivalent to *set/write* operation bring the sample to *on-state*. With positive pulses the HRS to LRS transition occurs and by this *reset* process the stored information is *erased* i.e. the sample returns to its *off-state*. Between each write and erase pulse, the resistance state of the sample was read with a voltage pulse of 0.1 V & 20 ms. The switching was reproducible and resistance states were stable for several months as tested. Contrast between the resistance states in this particular example is about 150 %.

Capacitor-like memory cells with Aluminum top-electrodes of size ~ 150 µm & thickness 1 µm were prepared to examine the switching at micron scale; see figure 3a. I-V measurements showed the PDR switching behaviour, and in the pulse-mode operation the LRS-HRS transition was demonstrated (with voltage pulses of amplitudes down to 1 V and pulse widths down to 1 µs) for hundred of cycles with resistance contrast of 100 % between the resistance states. An example of results obtained with Al top-electrodes is shown in figure 3b.

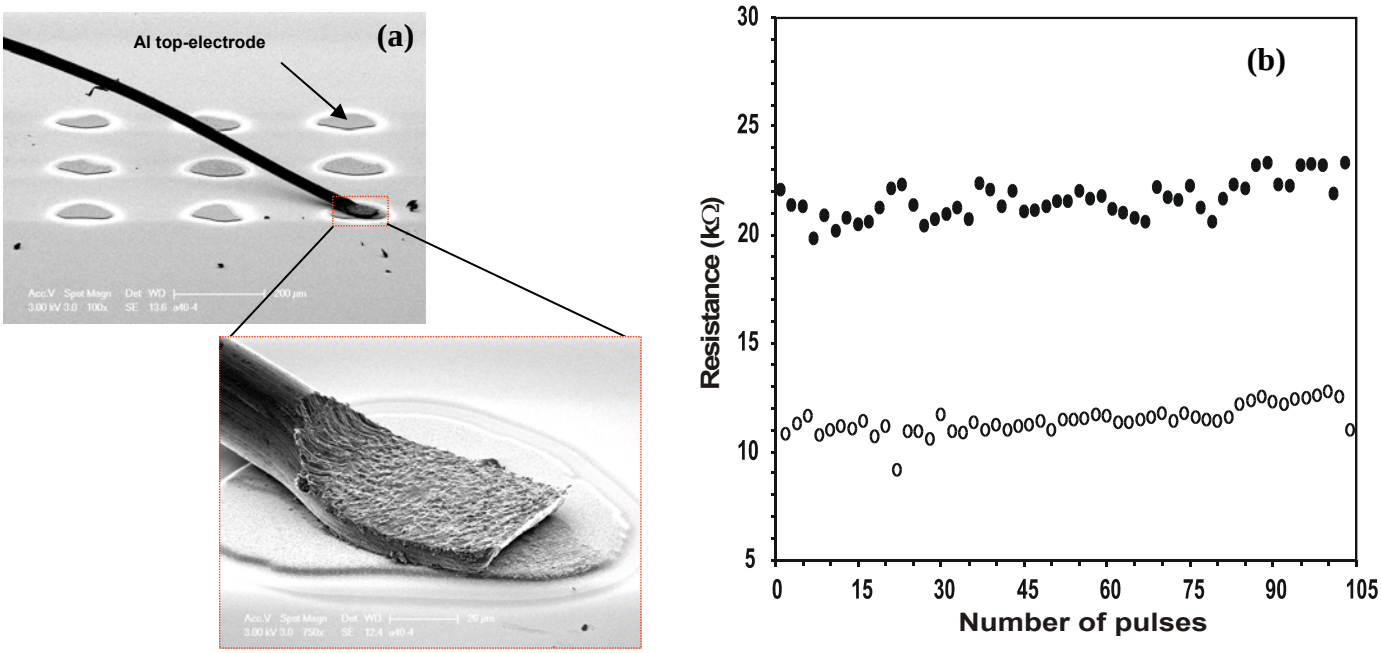

Figure 3. *(a) Capacitor-like cell structures with a 40 nm GST film and Al top-electrodes. (b) Low-Resistance States and High-Resistance States during the pulse-mode operation with voltage pulses of ±2 V and 1 µs.*

PDR switching studies using CAFM

Memory switching at nanoscales is essential to obtain high data-storage densities. In recent years, a strong impetus in this direction has been given by AFM nanolithography [15]. Therefore, we explored the resistance switching at nanoscales by CAFM and in this case the conductive AFM-tip with radius >50 nm, served as top electrode to the GST film. Figure 4a is a contact-mode AFM topograph showing an array of tip-written crystalline marks in an amorphous GST film. These marks were written by injecting DC voltage pulses of amplitude -5 V and width 500 ms from the tip into the electrically grounded film. The written marks are visible as pits at nanoscale because of the (local) density reduction of the amorphous film upon crystallization under the tip. One of the crystalline marks was considered to examine the PDR switching at nanoscale. Continuous scanning of an area including the mark with a positive bias voltage of 1.5 (i.e. the film is biased with respect to the virtually grounded tip), referred as a *set* operation, brought it into a LRS or *on-state*. On the other hand, a negative bias scanning (-1.5 V), referred as a *reset* operation, takes the mark to a HRS or *off-state*. When the *set* operation is repeatedly performed with +1.5 V, the mark switches back to its LRS or *on-state*. Simultaneous measurement of current flow through the tip during scanning allowed mapping the resistance state of the mark during the *set/reset* operations. The background amorphous phase resistance during these operations remains below the current detection limit (i.e. 5 pA) of our CAFM setup. Figures 4b, 4c & 4d are topographs of the mark during the *set*/*reset* operations. Figures 4e, 4f & 4g are current-images showing the LRS, HRS and LRS of the mark during the *set*, *reset* and *set* operations, respectively. Figures 4h, 4i & 4j are current-profiles corresponding to the current-images 4e, 4f & 4g, respectively.

Note that the HRS of the mark is electrically indistinguishable from the surrounding amorphous phase (cf. 4f & 4i), because the current flow across both is <5 pA and thus lower than the detection limit of the CAFM setup. During the *set*/*reset* operations topography of the mark did not alter markedly (cf. 4b, 4c & 4d), indicating that there is no structural change involved with the PDR switching. The ON-state current profiles, 4h & 4j, reveal that the mark has a resistance contrast of more than 3 orders of magnitude with its surrounding. The operating voltage required for this switching (±1.5 V) is clearly lower than the threshold voltage (> ±4 V) needed for inducing the amorphous-crystalline phase transition, indicating that the former type of switching is more advantageous for future device applications. Since the switching causes no detectable density changes, it should also be advantageous from the cyclability point of view. In current images, 4e & 4g, it can be seen that the electrical conductivity of the crystalline mark (within the dashed circle) is not uniform. A considerable area fraction is still at HRS, where it should be homogeneous at LRS. This is attributed to several factors, e.g. an incomplete crystallization by the tip, an improper tip-sample electrical contact due to relative fast tip scanning, surface roughness of the sample and removal of the conductive coating from the tip. Our experiments also prove that the switching is not limited by the switching area or the electrode material type, but the switching speed is limited by a few experimental constraints i.e., AFM scanning speed, and pulse-shape loss due to the large capacitance of our non-optimized test structures.

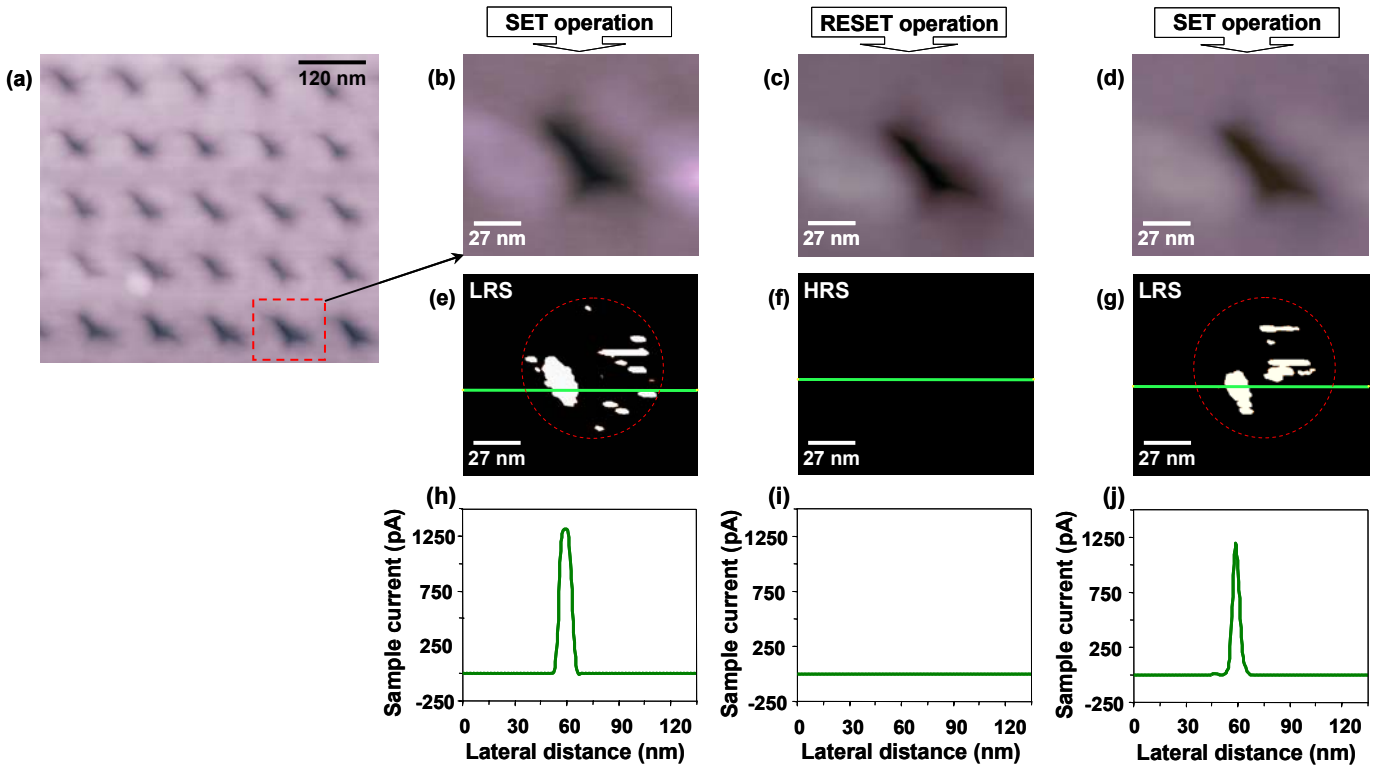

Figure 4. *PDR at nanoscales: (a) AFM topograph showing a tip-written crystalline bit pattern in a 40 nm amorphous GST film. (b), (c) & (d) are topographs of a crystalline mark during the set, reset and set operations, respectively. (e), (f) & (g) are current-images recorded with ±1.5 biasing voltage showing on-, off- and on-states of the mark, respectively. (h), (i) & (j) are on-, off- and on-state current profiles, corresponding to the current-images (e), (f) & (g), respectively.*

Proposed mechanism of PDR switching in chalcogenides

The resistance switching driven by the polarity of the applied electric field can be related to the solid-state electrolytic behavior of the chalcogenide. When it is subjected to an electric field, electrochemical reactions near the electrodes lead to ionic conduction. If the electric field is sufficiently strong, electrically conductive filamentary pathways form between the electrodes leading to an LRS, and if the polarity is reversed, the pre-existing paths become discontinuous due to ion migration in the opposite direction resulting in a HRS. In literature, chalcogenides showing this behavior include AgS [9], CuS [10], AgGeSe [11], AgGeTe [12], and AgInSbTe [13], where the LRS and HRS are a result of the formation and rupture of Ag- or Cu-filaments. A similar electrolytic switching mechanism probably holds for our Sb-excess GST chalcogenide material. In this case, conductive Sb- instead of Ag- or Cu-filaments can be formed and dissolved in amorphous phase that still persists with a small volume fraction when the GST crystallites are formed.

Points favoring of this mechanism are: (1) crystallization of this type of material leads to phase separation, where the stoichiometric nanosized $Ge_2Sb_2Te_5$ crystals form with the excess Sb as amorphous phase at the grain boundaries [16], and (2) cross-sectional transmission electron microscopy (TEM) studies showed that in GeSbTe films a strong tendency exists to form crystallites near the film surface leaving some amorphous volume near the film-substrate interface [17,18]. Note that (metallic) Sb is several orders of magnitude more conductive than Ge or Te within GST system. Therefore, when a sufficiently strong electric field is applied, conducting dendrite-like Sb-filaments form and can bridge the $Ge_2Sb_2Te_5$ grains through the amorphous matrix with the electrodes. The conducting Sb-bridges persist until they are dissolved/ruptured by reversing the polarity of the electric field. Instead of Sb-filaments also a similar (electrolytic) mechanism where grain-boundaries can switch between a conductive and insulating state can explain the observations.

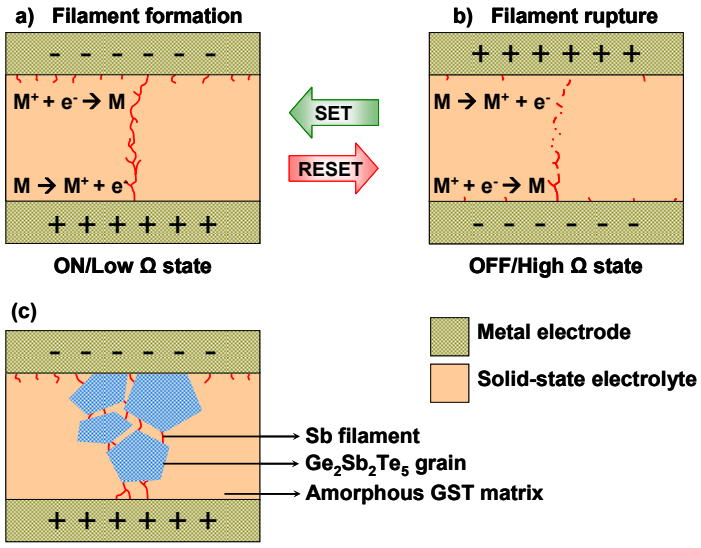

Figure 5. *Schematic representation of the polarity-dependent resistance switching mechanism in a solid-state electrolyte. (a) Filament formation due to SET operation: Metal ions are produced at the bottom (+ ive) electrode and migrate towards the top (- ive) electrode, where the neutral metal atoms accumulate. Due to these solid-state electrochemical reactions, dendrite-like conductive filamentary pathways form in the solid electrolyte material. This filament formation leads the material to a lower-resistance or ON-state. (b) Filament rupture due to RESET operation: The ions produced at the top (+ ive) electrode start to migrate towards the bottom (- ive) electrode, resulting in rupture of the existing conductive pathway(s), especially to a larger extend near the top electrode. At this stage new dendrites start to grow from the bottom electrode. The filament breakage brings the material into a higher-resistance or OFF-state. (c) Schematic diagram representing the formation of electrically conductive pathways in Sb rich $Ge_2Sb_{2+x}Te_5$ solid-state electrolyte layer. During SET operation, excess Sb at $Ge_2Sb_2Te_5$ grain boundaries form filaments electrically connecting the grains surrounded by amorphous phase with the electrodes. These Sb filaments remain until they are dissolved by a sufficiently high electric field with a reverse polarity.*

In order to verify the validity of the above mechanism, the most obvious experiment would be to remove the excess Sb and repeat the measurements examining the response to polarity reversal. Therefore, new exactly stoichiometric (40 nm thick) $Ge_2Sb_2Te_5$ films were deposited on the Si wafers covered by the Mo bottom electrodes. As top

electrodes the millimeter scale Ag electrodes were used. Subsequent measurements revealed that in these samples, electrically crystallized between the electrodes, PDR switching did not occur [19]. The *IV* characteristics of the cell did not show any evidence for a resistance switching behaviour (in-between +1 and -1 V). The sample-current linearly increases with the voltage sweep in both positive and negative directions (i.e., the sample resistance does not significantly change with the applied-voltage-polarity). No threshold-point in the applied voltage is detected at around 0.5 *V* as was observed for a 40 *nm* $Ge_2Sb_{2+x}Te_5$ film; see figure 2a. PDR switching was also not observed using a large number of pulses with the following characteristics: 1 µs ±1.25 V, 50 µs ±1.25 V, 1 µs ±1.5 V. See for an example figure 6. Only by exposing the cells to hundreds of relative long voltage pulses of ±1.5 V and 250 µs, it turned out possible to transform the $Ge_2Sb_2Te_5$ film into a state allowing signs of non-ideal PDR switching [19]. Probably the relatively harsh electro-thermal treatment leads to decomposition of the $Ge_2Sb_2Te_5$ such that PDR switching is not fully impossible anymore. However, the large difference between the excess-Sb and the stoichiometric $Ge_2Sb_2Te_5$ in their ability to demonstrate PDR switching proves that indeed the (excess metallic) Sb plays a crucial role in the switching process.

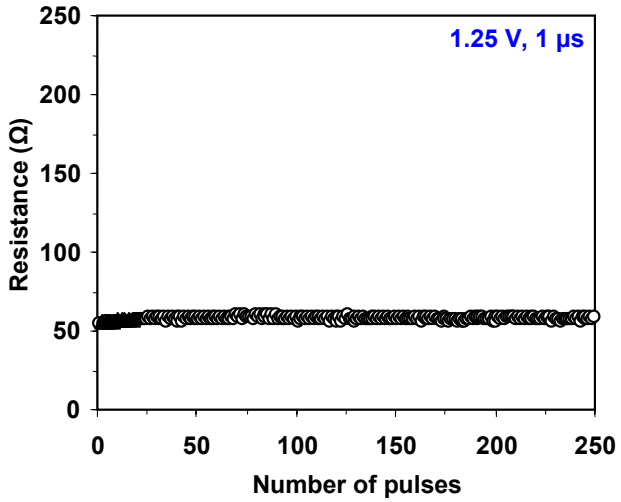

Figure 6. *Response of the cell-resistance to switching pulses of ±1.25 V and 1 µs. ▲: positive pulses; O : negative pulses. Polarity dependent resistance switching does not occur in this case of stoichiometric* $Ge_2Sb_2Te_5$ *but was observed under identical conditions in case of excess Sb* $Ge_2Sb_2Te_5$*; see Fig.2b.*

4. CONCLUSIONS

We demonstrated the existence of polarity-dependent resistance switching in crystallized Sb-excess $Ge_2Sb_2Te_5$ films at various length scales. In prototype capacitor-like cells with sizes down to the micrometer scale, voltage pulses showed this switching within time scales of micro-seconds with resistance contrasts up to 150% between the resistance states. Moreover, using conductive atomic force microscopy, switching was also possible at nanoscales with a better resistance contrast of three orders of magnitude. The electrical resistance switching behaviour is attributed to the solid-state electrolytic (ionic conducting) behaviour of the films, where the formation and rupture of electrically conductive Sb bridges between the crystallites and the electrodes are driven by the polarity of the applied electric field. Strong supports in favour of this mechanism are experimental results showing that the PDR switching turned out (nearly) impossible in stoichiometric $Ge_2Sb_2Te_5$. Notably, the switching (*write*/*erase*) voltages < ±1.5 V is fairly small compared to those used in current ferroelectric and flash memories and is also compatible with future microelectronic and data-storage systems. Our study shows conclusively that in a single material phase-change and polarity-dependent resistance switching can be combined.

REFERENCES

1. G.A. Prinz, Science **282**, 1660 (1998).
2. G.R. Fox, F. Chu, and T. Davenport, J. Vac. Sci. Technol. B. **19**, 1967 (2001).
3. S.R. Ovshinsky, Phys. Rev. Lett. **21**, 1450 (1968); K. Nakayama, K. Kojima, F. Hayakawa, Y. Imai, A. Kitagawa, and M. Suzuki, Jpn. J. Appl. Phys. I **39**, 6157 (2000); S. Lai and T. Lowrey, Tech. Dig. – Int. Electron Devices Meet. **2001**, 803; F. Pellizzer *et al*., Proc. of the 2004 IEEE Symp. on VLSI Technology, Digest of Technical Papers, Paper No. 3.1, p. 18; S.H. Lee, Y.N. Hwang, S.Y. Lee, K.C. Ryoo, S.J. Ahn, H.C. Koo, C.W. Jeong, Y.-T. Kim, G.H. Koh, G.T. Jeong, H.S. Jeong and K. Kim, Proc. of the 2004 IEEE Symp. on VLSI Technology, Digest of Technical Papers, p. 20.
4. K.L. Chopra, J. Appl. Phys. **36**, 184 (1965).
5. A. Beck, J.G. Bednorz, Ch. Gerber, C. Rossel, and D. Widmer, Appl. Phys. Lett. **77**, 139 (2000).
6. A. Sawa, T. Fujii, M. Kawasaki, and Y. Tokura, Appl. Phys. Lett. **85**, 4073 (2004).
7. X. Chen, N. Wu, J. Strozier, and A. Ignatiev, Appl. Phys. Lett. **89**, 063507 (2006); A. Ignatiev, N.J. Wu, X. Chen, S.Q. Liu, C. Papagianni, and J. Strozier, Phys. Stat. Sol. (b) **243**, 2089 (2006).
8. K. Szot, R. Dittmann, W. Speier, and R. Waser, Phys. Stat. Sol. (RRL) **1**, R86 (2007).
9. Y. Hirose and H. Hirose, J. Appl. Phys. **47**, 2767 (1976); K. Terabe, T. Hasegawa, T. Nakayama, and M. Aono, Nature **433**, 47 (2005).
10. T. Sakamoto, NEC J. of Adv. Tech. **2**, 260 (2005).
11. M.N. Kozicki, M. Park, and M. Mitkova, IEEE Trans. Nanotechnol. **4**, 331 (2005).
12. C.-J. Kim and S.-G Yoon, J. Vac. Sci. Technol. B **24**, 721 (2006).
13. Y. Yin, H. Sone, and S. Hosaka, Jpn. J. Appl. Phys. **45**, 4951 (2006).
14. A.L. Greer and N. Mathur, Nature **437**, 1246 (2005).
15. S. Gidon, O. Lemonnier, B. Rolland, O. Bichet, C. Dressler, and Y. Samson, Appl. Phys. Lett. **85**, 6392 (2004); K. Tanaka, J. Non-Cryst. Solids **353**, 1899 (2007); C. D. Wright, M. Armand, and M. M. Aziz, J. Hist. Astron. **5**, 50 (2006).
16. N. Yamada and T. Matsunaga, J. Appl. Phys. **88**, 7020 (2000).
17. S.-M. Yoon, K.-J. Choi, N.-Y. Lee, S.-Y. Lee, Y.-S. Park, and B.-G. Yu, Jpn. J. Appl. Phys., Part 2 **46**, L99 (2007).
18. J. A. Kalb, C. Y. Wen, F. Spaepen, H. Dieker, and M. Wuttig, J. Appl. Phys. **98**, 054902 (2005); T. H. Jeong, M. R. Kim, and H. Seo, *ibid*. **86**, 774 (1999).
19. R. Pandian, B. J. Kooi, G. Palasantzas, J. T. M. De Hosson and A. Pauza, Submitted for publication.

Biography Dr. Ir. B.J. Kooi

Associate professor in Materials Science group, Dept. Applied Physics, Zernike Institute for Advanced Materials, University of Groningen, The Netherlands.

Jan. 1991- Jan.1995: Ph.D. student in the section 'Physical Chemistry of the Solid State' headed by prof. dr. ir. E.J. Mittemeijer, Laboratory for Materials Science, Delft University of Technology, The Netherlands.

Research: Published over 130 papers in international scientific journals and proceedings.

Main interests: Phase change materials, nanostructured materials, interfaces, boundaries, segregation, precipitation and phase transformations including nucleation and growth using as main experimental technique (in-situ, high-resolution and analytical) Transmission Electron Microscopy.